© 2022. This manuscript version is made available under the CC-BY-NC-ND 4.0 license: http://creativecommons.org/licenses/by-nc-nd/4.0/

A study of the inclusion complex formed between cucurcubit[7]uril and 1-[4-(dimethylamino)phenyl]-ethanone

Xian-Hao feng,[a] Zhi-ChaoYu,[a] Wei Zhang,[a] Carl Redshaw,[b] Timothy J. Prior,[b] Tie-Hong Meng[c], Chun-Rong Li[c],Zhu Tao,[a] Xin Xiao,*[a]

[a] Key Laboratory of Macrocyclic and Supramolecular Chemistry of Guizhou Province, Guizhou University, Guiyang 550025, China.

[b] Department of Chemistry, University of Hull, Hull HU6 7RX, U.K.

[c] Public Course Teaching Department, Qiannan Medical College for Nationalities, Duyun, 558000, China.

E-mail: gyhxxiaoxin@163.com (X. Xiao)

Abstract: In the work, we have studied the interaction of cucurbit[7]uril (Q[7]) with 1-[4-(dimethylamino)phenyl]-ethanone (DAPE) using a variety of techiniques including ^{1}H NMR spectroscopy, UV-vis adsorption and fluorescence spectroscopies, Isothermal titration calorimetry and single crystal X-ray diffraction. Results revealed the formation of a 1:1 complex, whilst the molecular structure of the species $[(Q[7]@DAPE)Ca(H_2O)_3]_2(CdCl_4)_2\cdot 31(H_2O)$ is reported.

Keywords: Cucurbit[7]uril; 1-[4-(dimethylamino)phenyl]-ethanone; host-guest complex; structure.

Introduction

Cucurbit[*n*]urils (Q[*n*]s, where n = 5 to 15) are a relatively new class of macrocycles that are readily available from the acid catalyzed condensation of glycoluril and formaldehyde. [1-5] Q[*n*]s have a highly symmetric structure with good structural rigidity and hydrophobicity, and the electrical neutrality of their cavities allows them to encapsulate small guest molecules. [6-9] In addition, the carbonyl unit located at the portals of Q[*n*]s possesses a significant negative potential, giving it multiple sites of action. [10-14] The hydrophobic cavities of Q[*n*]s are the main object of study in cucurbit[*n*]urils chemistry, which has led to extensive studies on the host-guest chemistry of Q[*n*]s. [15-17] Q[7] in particular has been found to exhibit excellent affinities towards certain guests, particularly amino-containing substrates, but for the cucurbit[*n*]uril family, there are not many host-guest crystal structures reported for the Q[7] system [18]. We have also been studying the host-guest chemistry of Q[7], and have reported a number of systems including the use of amines as the guest. [19]

Herein, we extend our studies to the guest 1-[4-(dimethylamino)phenyl]-ethanone (also known as P-acetyl-*N*,*N*-dimethylaniline; 4-dimethylaminoacetophenone) [20], and abbreviated herein as DAPE. Our interest in DAPE originates from the fact that DAPE is an important intermediate in organic synthesis and pharmaceuticals. Moreover, it is also known to irritate the eyes, respiratory system and skin[21]. Cucurbit[*n*]urils have been shown to act as a drug carrier[22-23], whilst in other studies we and others have shown have encapsulation of a guest (e.g. a pesticide) can allow for control of properties such as toxicity [24]. In recent years, cucurbit[*n*]uril assemblies have been involved in many research fields, such as chemistry, materials, environment and biology, and have attracted wide attention [25-29]. Supramolecular assembly systems with novel structures, good rigidity and different properties have been constructed by selecting different construction modes through intermolecular hydrogen bonding, induced dipole, π--π and other weak interactions.

Herein, we constructed a supramolecular system between DAPE and Q[7]; there are few reports regarding the use of DAPE and supramolecular self-assemblies. Matsushita *et al*. [30] have reported the interaction between α-, β- and γ-cyclodextrins

(CD) and DAPE, and studied the fluorescent properties, and the results show that the cavity size affects the optical properties of DAPE. Fluorescence properties of excited DAPE complexed with α-cyclodextrin (CD) have been studied [31]. The complex exhibited dual fluorescence in neutral aqueous solution and no TICT fluorescence was observed under alkaline conditions. In this paper, the optical properties of DAPE and Q[7] have been subjected to a preliminary study in order to provide a reference for the subsequent study of DAPE and larger ring systems. However, supramolecular recognition of DAPE by cucurbit[*n*]urils has not been reported. Therefore, the supramolecular assembly mode of DAPE and cucurbit[*n*]urils was constructed herein, and a crystal structure of the 1:1 host-guest complex was obtained. The hydrophobic cavity associated with cucurbit[*n*]urils can reduce the fluorescence of DAPE. Given all of the above, this work will provide new insight into cucurbit[*n*]urils as a drug carrier for DAPE. Scheme 1 shows the structures of Q[7] and DAPE.

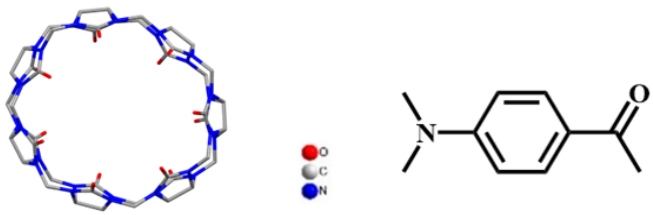

Q[7] DAPE

Scheme 1. Structures of Q[7] and DAPE.

Experimental section

Materials

The guest 1-[4-(dimethylamino)phenyl]-ethanone was obtained from Aladdin (Shanghai, China). Q[7] was prepared and purified according to the literature method. [32] All other reagents were of analytical reagent grade and were used without any further purifification. Deionized water was used in all experiments.

^{1}H NMR spectroscopy

All the ^{1}H NMR spectra, including those for the titration experiments, were recorded at 298.15 K on a JEOL JNM-ECZ400S 400 MHz NMR spectrometer (JEOL) in D_2O. D_2O was used as a field-frequency lock and the observed chemical shifts are reported in parts per million (ppm) relative to that for the internal standard (TMS at 0.0 ppm).

In order to investigate the complexation of Q[7] with 1-[4-(dimethylamino)phenyl]-ethanone in solution, ^{1}H NMR spectroscopic titration experiments were performed by adding increasing amounts of Q[7] to the solution of 1-[4-(dimethylamino)phenyl]-ethanone in D_2O.

UV-Vis absorption spectroscopy

The UV-vis absorption spectra of the host-guest complexes were recorded using an Agilent 8453 spectrophotometer at room temperature. The aqueous solution of 1-[4-(dimethylamino)phenyl]-ethanone was prepared at a concentration of 1.0×10^{-3} mol·L^{-1}. An aqueous solution of Q[7] was prepared with a concentration of 1.0×10^{-3} mol·L^{-1} for the absorption spectra determination. The UV-vis absorption experiments were performed as follows: 200 μL of a 1.0×10^{-3} mol·L^{-1} stock solution of 1-[4-(dimethylamino)phenyl]-ethanone and various amounts of an aqueous 1.0×10^{-3} mol·L^{-1} Q[7] solution were transferred into a 10 mL volumetric flask, and then the volumetric flask was filled to the final volume with distilled water. Samples of these solutions were combined to give solutions with an $N_{Q[7]}/N_{DAPE}$ = 0, 0.1, 0.2, 0.3, . ., and 2.0. The Job's plot method was used to determine the inclusion ratio of the substance, $N_{DAPE}/(N_{Q[7]} + N_{DAPE})$ = 0, 0.1, 0.2, 0.3, . . ., 1.0.

Fluorescence spectroscopy

The binding behavior between Q[7] and AC was initially studied by employing UV-vis absorption and fluorescence spectroscopy. The gradual addition of Q[7] results in a gradual decrease in the maximum absorbance of 1-[4-(dimethylamino)phenyl]-

ethanone (at a fixed 1-[4-(dimethylamino)phenyl]-ethanone concentration of 2×10^{-5} $mol\cdot L^{-1}$) at 345 nm (Fig. 1A) until the ratio of the host-guest reached 1. This suggests a 1:1 host-guest inclusion complex is formed between the Q[7] and 1-[4-(dimethylamino)phenyl]-ethanone.

Isothermal titration calorimetry (ITC) experiment

To further understand the nature of the host-guest complexation of Q[7] with 1-[4-(dimethylamino)phenyl]-ethanone, we carried out isothermal titration calorimetry (ITC) experiments. The obtained thermodynamic parameters reveal that the host-guest complexation is both enthalpically and entropically favorable ($n = 0.942 mol^{-1}$, $\Delta H = -55.35\ kJ\cdot mol^{-1}$, $T\Delta S = -31.05\ kJ\cdot mol^{-1}$, $\Delta G = -24.30\ kJ\cdot mol^{-1}$, $\Delta S = -105.9\ J\cdot mol^{-1}$). In addition to the ion-dipole interactions between the positively charged nitrogens on the 1-[4-(dimethylamino)phenyl]-ethanone guest and the oxygen atoms on the portals of the Q [7] host, van der Waals interactions between the surfaces of the 1-[4-(dimethylamino)phenyl]-ethanone guest and the inner wall of the Q[7] host contribute favorable enthalpy for the host-guest complexation. The removal of the water molecules from the Q[7] cavity and the Q[7] portals, and from the solvated shell of the 1-[4-(dimethylamino)phenyl]-ethanone is likely responsible for this favorable entropic gain. According to the van't Hoff equation ($\ln K = -\Delta H /RT + \Delta S /R$) and the enthalpic andentropic values, a large binding constant $(2.212 \pm 0.2) \times 10^4$ of Q [7] with 1-[4-(dimethylamino)phenyl]-ethanone was obtained, which is consistent with the UV-vis data.

Single-crystal X-ray crystallography

Single-crystal data for compound **1** were collected on the Bruker D8 VENTURE diffractometer with graphite monochromatic Mo-Kα radiation (λ = 0.71073 Å). Empirical absorption corrections were applied by using the multi-scan multiscan program SADABS. Structural solution and full matrix least-squares refinement based on F^2 were performed within the program Olex2. [33]Anisotropical thermal parameters

were applied to all the non-hydrogen atoms. All hydrogen atoms were treated as riding atoms with an isotropic displacement parameter equal to 1.2 times that of the parent atom. Disordered solvent was modelled using a solvent mask within Olex2.

Preparation of complex **1**

Q[7] (6.71 mg, 0.005 mmol) was added to a solution of 1-[4-(dimethylamino)phenyl]-ethanone (8.2 mg, 0.05 mmol) and $CdCl_2$ (9.2 mg, 0.05 mmol) and $CaCl_2$ (5.5 mg, 0.05 mmol) in HCl solution (5 mL, 3 $mol \cdot L^{-1}$). The mixture was heated until complete dissolution. Following slow evaporation of the volatiles from the solution over a period of about three days, block colorless crystals of complex **1** were obtained.

Results and discussion

^1H NMR titration experiments were employed to investigate the interaction between Q[7] and the potential guest DAPE. As shown in Figure 1, on gradually adding Q[7], the entire microenvironment of DAPE began to change, which was evident from the chemical shifts associated with DAPE. For example, H_2 H_3 and H_4 of the phenyl and methyl groups attached to the ethanone of DAPE shifted due to the shielding effect of the cavity with δ_2 = 6.85 to 6.61ppm, δ_2 = 7.80 to 7.21 and δ_4 = 2.40 to 2.21 ppm. These shifts indicate that the pyridine and methyl groups are accommodated within the cavity of Q[7]. Meanwhile, H_1 on the dimethylamine group only experienced a slight upfield shift from δ = 2.93 to 2.90 ppm. Thus, it can be inferred that the whole guest molecule resides inside the cavity of Q[7], which is consistent with the single-crystal structure *vide infra*.

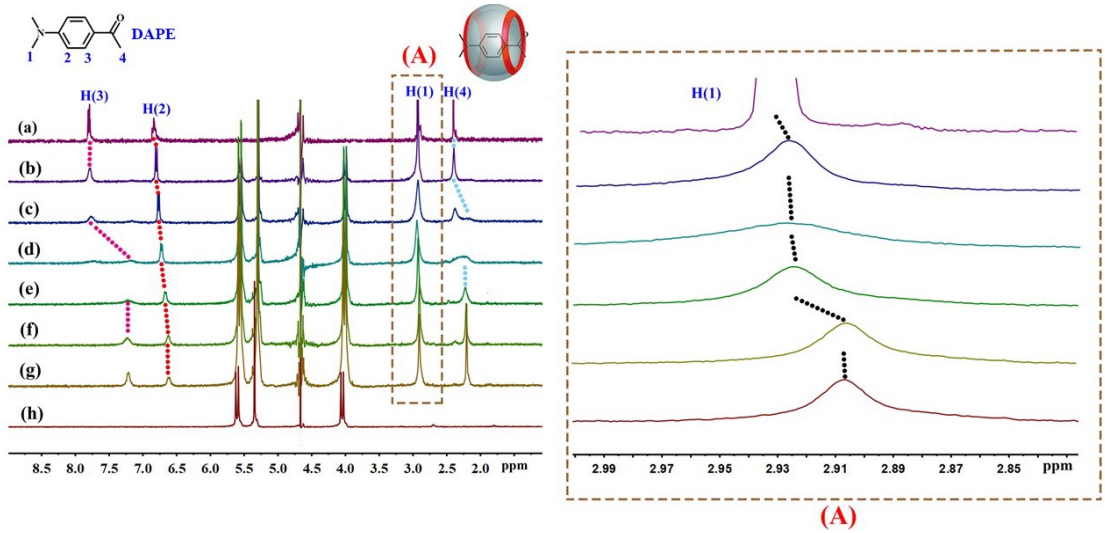

Figure 1. Interaction of DAPE and Q[7] (20 °C): (a) ^{1}H NMR spectra (400MHz, D_2O) of DAPE (*ca*. 0.5 mM) in the absence of Q[7]; (b) in the presence of 0.10 equiv. of Q[7]; (c) in the presence of 0.20 equiv. of Q[7]; (d) in the presence of 0.40 equiv. of Q[7]; (e) in the presence of 0.6 equiv. of Q[7]; (f) in the presence of 0.8 equiv. of Q[7]; (g) in the presence of 1.0 equiv. of Q[7]; (h) and neat Q[7].

The system was also monitored via the use of UV-vis spectroscopy. Figure 2 shows the variation in the UV spectra obtained for aqueous solutions containing a fixed concentration of DAPE (3×10^{-5} mol·L^{-1}) and variable concentrations of Q[7]. The absorption band of the guest DAPE exhibits a decrease of the absorption peak at 345 nm on addition of Q[7]. The data for absorbance (A) *vs*. the ratio of the number of moles (N) of the host Q[7] and guest DAPE (DAPE /Q[7]) can be fitted by a 1:1 binding model. Furthermore, the Job's plot (Figure 2c) was consistent with the formation of a 1:1 host@guest complex.

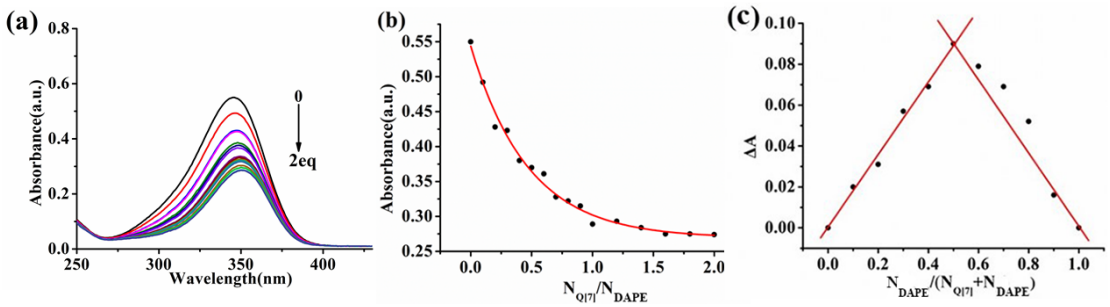

Figure 2. (Color online) (a) Electronic absorption of DAPE (3×10^{-5} mol·L^{-1}) upon addition of increasing amounts (0, 0.2, 0.4……1.6, 1.8, 2.0 equiv.) of Q[7]; (b) the concentrations and absorbance *vs*. $N_{Q[7]}/N_{DAPE}$ plots; (c) Continuous variation Job's plot for Q[7] and the guest on the basis of UV-vis titration spectra.

Fluorescence spectroscopy was further performed, and as shown in Figure 3, the guest, DAPE, exhibited an emission peak at 411 nm. Fluorescence titration experiments were further used to demonstrate the interaction ratio of Q[7] with DAPE. The fluorescence intensity associated with DAPE in aqueous solution decreased after the gradual addition of Q[7] (Figure 3a), and was accompanied by the generation of the blue shift phenomenon (from 411 nm to 391 nm). With the continuous addition of Q[7], when the stoichiometric ratio of Q[7]:DAPE was 1:1, the change in the fluorescence intensity of the system tended to be weaker, and the whole system reached equilibrium (Figure 3b). This is consistent with that deductions from the UV-vis absorption spectra as detailed above.

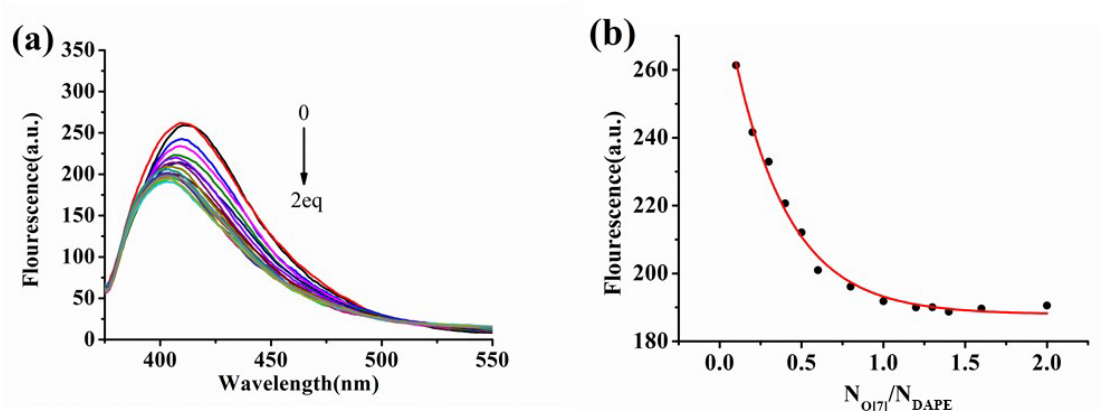

Figure 3. Titration fluorescence spectra of DAPE (3×10^{-5} mol·L^{-1}) (0, 0.1, 0.2,⋯2.0 equiv.). (a) Emission spectra; (b) change in fluorescence intensity with $N_{Q[7]}/N_{DAPE}$.

To shed light on the thermodynamic parameters associated with the complexation between Q[7] and DAPE, ITC experiments were performed at 298.15 K (Figure 4, Table 1). From the titration curve/experimental data, a K_a value of 2.14×10^4 M^{-1} was

calculated, together with a negative enthalpy variation value of ΔH^o = -55.35 KJ·mol^{-1}, and a negative entropy variation value of $T\Delta S^o$ = -31.03 KJ·mol^{-1}. This data suggests that the inclusion complex formation is driven by favorable enthalpy change accompanied by an unfavorable entropy change.

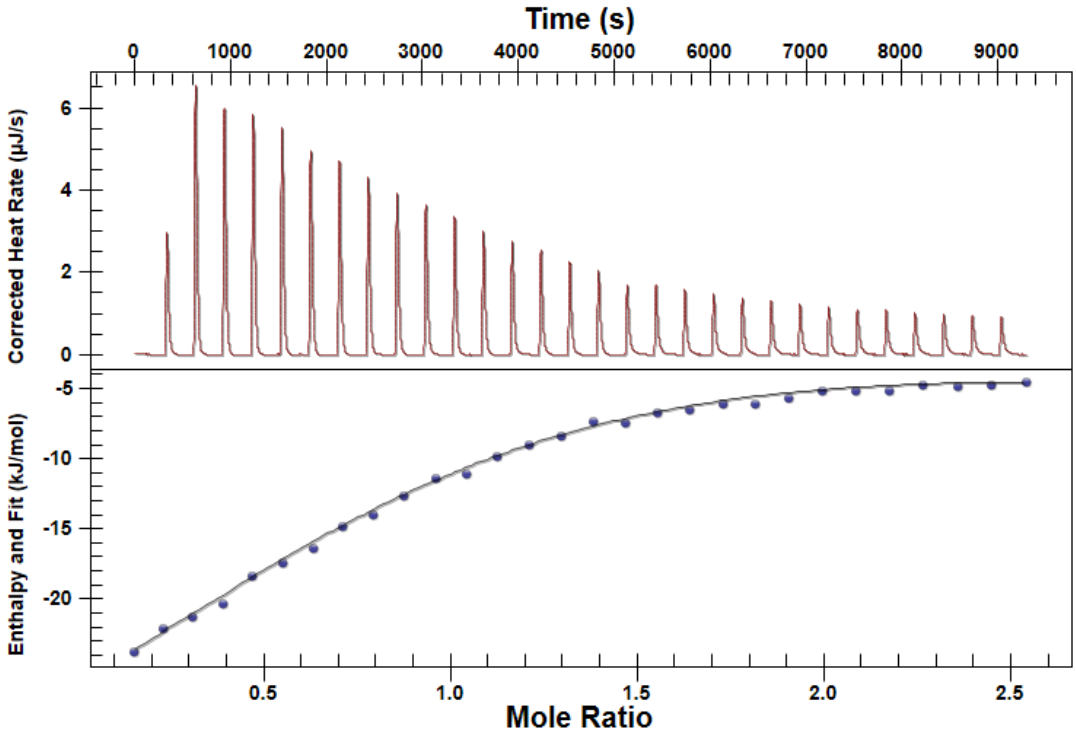

Figure 4. ITC profile of host Q[7] with guest DAPE at 298.15K.

Table 1. ITC measurements of the thermodynamics of Q[7]@ DAPE interaction at 298.15 K

Experiment	Q[7]@ DAPE
Ka (M^{-1})	2.14×10^4
ΔH (kJ·mol^{-1})	-55.35
$T\Delta S$ (kJ·mol^{-1})	-31.05
ΔG (kJ·mol^{-1})	-24.30
ΔS (kJ·mol^{-1})	-105.9
n	0.942

Molecular structure determination

Q[7]-DAPE crystallises in the centric space group $P2_1/n$ with a single Q[7] and the guest molecule 1-[4-(dimethylamino)phenyl]-ethanone present in the asymmetric unit, along with a single $[CdCl_4]^{2-}$ ion and one Ca^{2+} ion and both bound and unbound water. The guest molecule lies almost exactly perpendicular to the plane of the Q[7] ring and is centred within it rather than being displaced towards one side. On one face of the Q[7] ring a calcium ion is bound by two oxygens (Ca1 to O13 and O14 distances are 2.407(2) and 2.431(2) Å respectively). The guest molecule is bound to Ca1 *via* O15 and there are three molecules of water bound to Ca1. The centre of symmetry generates another identical Q[7] and guest. The second Q[7] binds to the Ca1 *via* O10 (Ca1–$O10^i$ is 2.522(2) Å, where $i = 1-x, 1-y, 1-z$), so that each Ca ion is 7-coordinate. There hydrogen bonds between two of the bound water molecules and the second symmetry equivalent Q[7]. The overall effect is to generate face-on dimers of Q[7]+guest that are akin to sandwiches with $2\times[Ca(H_2O)_3]^{2+}$ as the filling. Between these dimers are located $[CdCl_4]^{2-}$ anions and there are C–H···Cl interactions with the Q[7] molecules. The effect of these intermolecular interactions is to assembly the cationic dimers and anions into sheets that run parallel to the (1,0,-1) plane. There is further space between these layers that is occupied by disordered water and this was modelled using a solvent mask with Olex2. [33] Within the unit cell the void volume was 2017 $Å^3$ (24.8 % of unit cell volume) and this was occupied by electron density 624 e^- per cell, consistent with 62 water molecules per cell, with volume of 3.2 $Å^3/e^-$.

A representation of a single dimer is shown below (Figure 5) and further representations of the structure are located in the supporting information (Figures S1-S3).

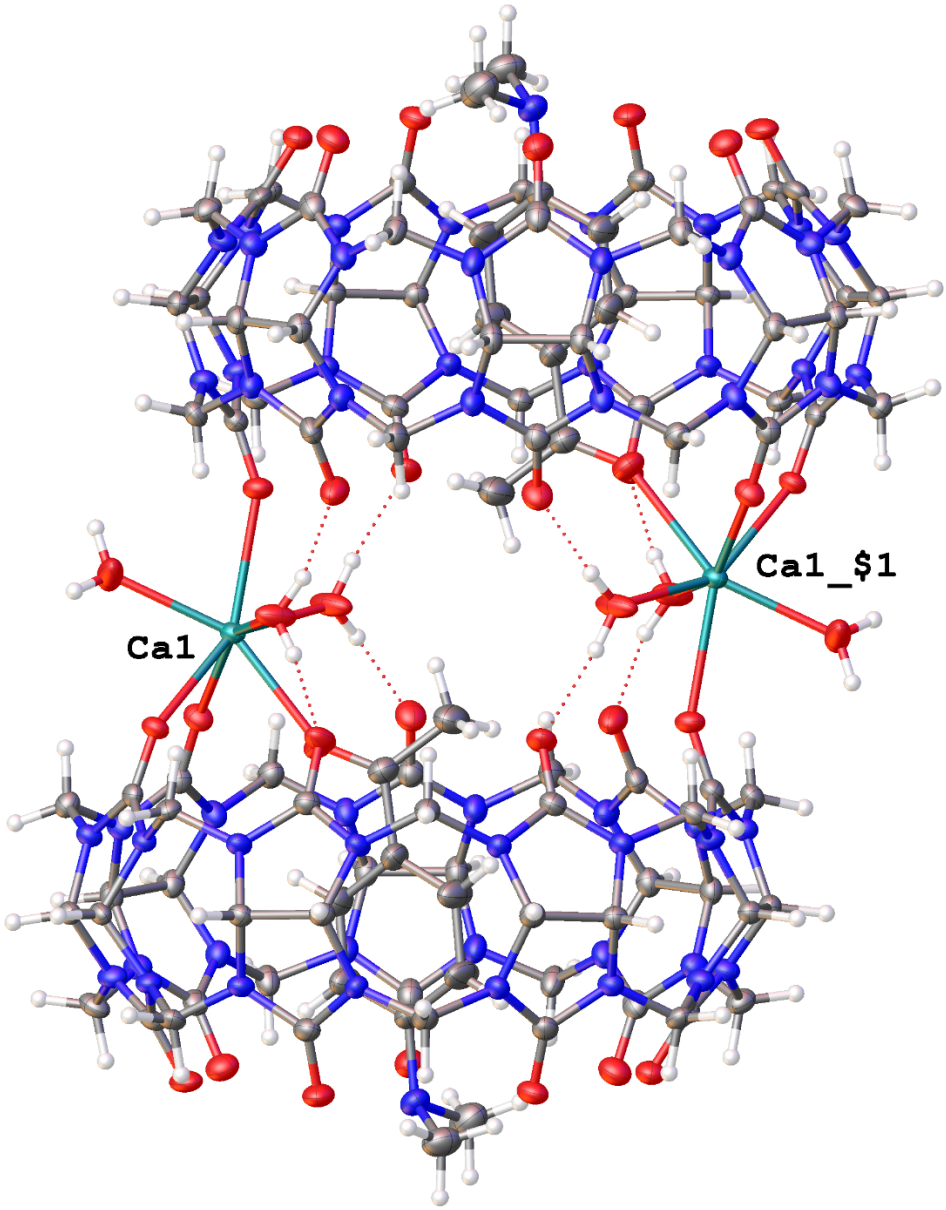

Figure 5. Dimeric unit of (Q[7]-DAPE.Ca$(H_2O)_3)_2$ with atoms drawn as 30% probability ellipsoids. Symmetry operation used to generate equivalent atoms: \$1 = 1−*x*, 1−*y*, 1−*z*.

As shown in Figure 6, in the sandwich structure, the carboxyl oxygen of Q[7] in one complex forms hydrogen bonds with a water molecule and this water molecule also hydrogen bonds with the carbonyl oxygen of another complex. Hydrogen bonding interactions, such as O(12)···O(16)···O(9); O(8)···O(17)···O(11) are observed with bond lengths between 2.696 and 2.788 Å. These hydrogen bonds further strengthen the stabilization of the sandwich structure. Moreover, two adjacent dimers form a one-dimensional assembled host-guest supramolecular structure via hydrogen-bonding interactions between the portal carbonyl oxygen atom O2 of Q[7] and the coordinating

water molecule O18; the distance O(5)–H···O(18) is 1.939 Å.

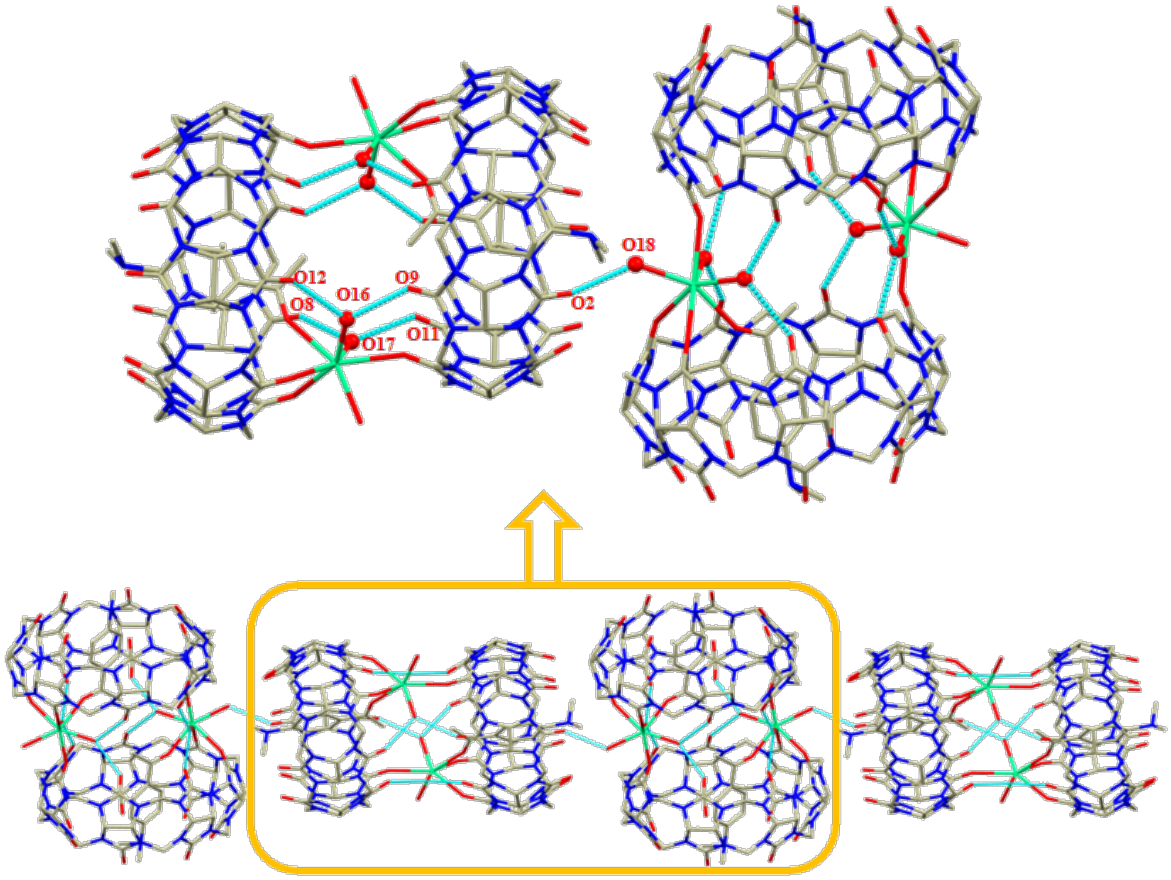

Figure 6. One-dimensional supramolecular chain of Q[7]-DAPE.

In the crystal stacking diagram of complex Q[7]-DAPE along the *a*-axis direction (figure 7), one-dimensional supramolecular chains are observed in a layered arrangement parallel to each other, thereby forming a two-dimensional network; the $[CdCl_4]^{2-}$ anion is trapped in a channel surrounded by four dimers.

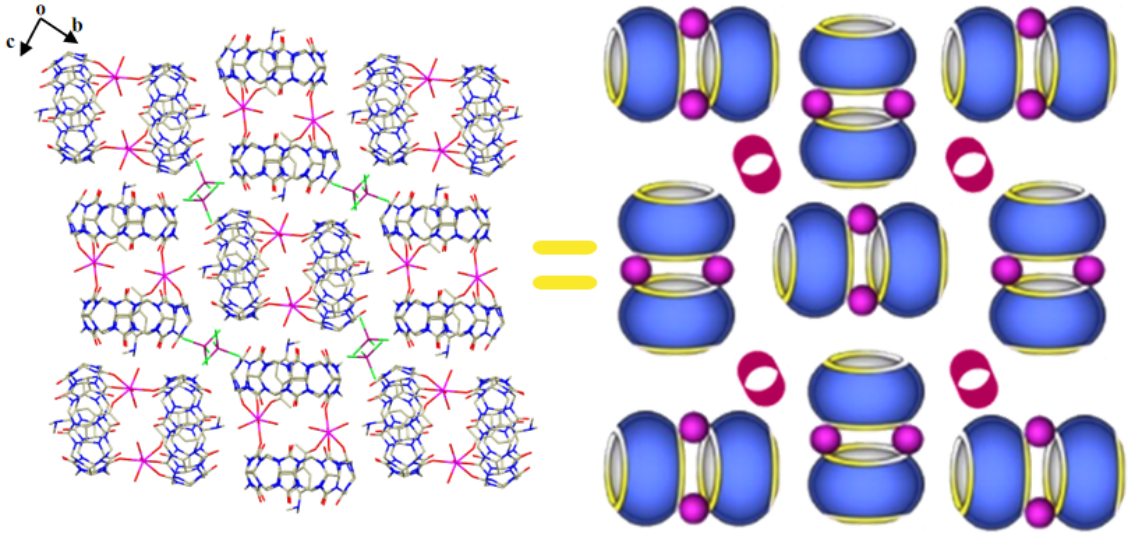

Figure 7. Two-dimensional network of Q[7]-DAPE viewed down the *a* axis.

In conclusion, we have studied the interaction of cucurbit[7]uril (Q[7]) with 1-[4-(dimethylamino)phenyl]-ethanone (DAPE) in the presence of $CdCl_2$ and $CaCl_2$, and find that in solution, data is consistent with a 1:1 inclusion complex. A crystal structure determination revelaed that in the solid state, a dimer is formed involving bridging calcium units. Extensive hydrogen bonding results in the formation a 2D network.

Conclusion

In summary, the results herein reveal that Q[7] can simultaneously hold one molecule of 1-[4-(dimethylamino)phenyl]-ethanone in the hydrophobic cavity. We have characterized the 1:1 inclusion complex by a series of means such as NMR spectroscopy, X-ray crystallography, fluorescence spectroscopy and UV-Vis absorption spectra. Our research shows the driving force for the formation of highly stable inclusion complex is the weak interactions between guest and host, such as C-H···π, C-H···O, and the ion-dipole interactions between the inorganic metal anions and the host-guest complex.

Appendix 1. Supplementary data

CCDC 2160776 contains the supplementary crystallographic data for this paper. Copies of the data can be obtained free of charge on application to the CCDC, 12 Union Road, Cambridge CB2 1EZ, U.K. (email: deposit@ccdc.cam.ac.uk).

Empirical formula	$C_{104}Ca_2Cd_2Cl_8H_{184}N_{58}O_{67}$
Formula weight	3907.64
Temperature/K	298
Crystal system	monoclinic
Space group	*P21/n*
a/Å	16.0926(11)
b/Å	22.8025(16)
c/Å	23.0948(14)
α/°	90
β/°	106.013(2)
γ/°	90
Volume/$Å^3$	8145.8(9)
Z	2
$\rho_{calc}g/cm^3$	1.593
μ/mm^{-1}	0.564
F(000)	4044.0
Crystal size/mm^3	0.21 × 0.15 × 0.12
Radiation	MoKα (λ = 0.71073)
2Θ range for data collection/°	4.438 to 50.052
Index ranges	-19 ≤ h ≤ 19, -27 ≤ k ≤ 27, -27 ≤ l ≤ 27
Reflections collected	183734
Independent reflections	14375 [Rint = 0.0964, Rsigma = 0.0359]
Data/restraints/parameters	14375/211/998
Goodness-of-fit on F^2	1.014
Final R indexes [I>=2σ (I)]	R1 = 0.0444, wR2 =0.1049
Final R indexes [all data]	R1 = 0.0682, wR2 = 0.1201
Largest diff. peak/hole / e $Å^{-3}$	1.21/-0.74

Appendix 1. Crystallographic data for $[(Q[7]@DAPE)Ca(H_2O)_3]_2(CdCl_4)_2 \cdot 31(H_2O)$.

Acknowledgements

This work was supported by the Innovation Program for High-level Talents of Guizhou Province (No. 2016-5657) and the Science and Technology Fund of Guizhou Province ([2020]1Y051). CR thanks the EPSRC for an Overseas Travel Grant (EP/R023816/1).

References

[1] R. Behrend, E. Meyer, F. Rusche, *Justus Liebigs Ann. Chem*. 339 (1905) 1.

[2] W. A. Freeman, W. L. Mock, N. Y. Shih, *J. Am. Chem. Soc*. 103 (1981) 7367–7368.

[3] J. Kim, I. S. Jung, S. Y. Kim, E. Lee, J. K. Kang, S. Sakamoto, K. Yamaguchi, K. Kim, *J. Am. Chem. Soc*. 122 (2000) 540–541.

[4] A. I. Day, R. J. Blanch, A. P. Arnold, S. Lorenzo, G. R. Lewis, I. Dance, *Angew. Chem., Int. Ed*. 41 (2002) 275–277.

[5] X. J. Cheng, L. L. Liang, K. Chen, N. N. Ji, X. Xiao, J. X. Zhang, Y. Q. Zhang, S. F. Xue, Q. J. Zhu, X. L. Ni, Z. Tao, *Angew. Chem., Int. Ed*. 52 (2013) 7252–7255.

[6] W. Zhang, Y. Luo, J. Zhao, W.-H. Lin, X.-L. Ni, Z. Tao. *t*Q[14]-based AIE Supramolecular Network Polymers as Potential Bioimaging Agents for the Detection of Fe^{3+} in Live HeLa Cells, *Sensors and Actuators B-Chemical*, 354 (2011) 131189.

[7] M. Liu, J. Kan, Y. Yao, Y. Zhang, B. Bian, Z. Tao, Q. Zhu. Facile preparation and application of luminescent cucurbit[10]uril-based porous supramolecular frameworks, *Sensor Actuat B: Chem.*, 283 (2019) 290-297.

[8] H. Wu, J. Zhao, X. N. Yang, D. Yang, L. X. Chen, C. Redshaw, L. G. Yang, Z. Tao. A cucurbit[8]uril-based probe for the detection of the pesticide tricyclazole, *Dyes and Pigments*, 199 (2022) 110076.

[9] M. Liu, L. Chen, P. Shan, C. Lian, Z. Zhang, Y. Zhang, Z. Tao. Pyridine Detection Using Supramolecular Organic Frameworks Incorporating Cucurbit[10]uril, *ACS Appl. Mater. Inter.*, 13 (2021) 7434−7442

[10] D. Yang, M. Liu, Z. Tao. Polymeric self-assembled cucurbit[n]urils: Synthesis, structures and applications, *Coordin. Chem. Rev.*, 43 (2021) 213733

[11] W.-T. Xu, Y. Luo, W.-W. Zhao, M. Liu, G.-Y. Luo, Y. Fan, R.-L. Lin, Z. Tao. Detecting Pesticide Dodine by Displacement of Fluorescent Acridine from Cucurbit[10]uril Macrocycle, *J. Agric. Food Chem.*, 69 (2021) 584-591.

[12] Y. Luo, W. Zhang, M. Liu, J. Zhao, Y. Fan, B. Bian, Z. Tao. A supramolecular fluorescent probe based on cucurbit[10]uril for sensing the pesticide dodine, *Chinese*

Chem. Lett., 32 (2021) 367–370.

[13] M. Liu, M. Yang, Y. Yao, Y. Zhang, Y. Zhang, Q. Zhu, B. Bian. Specific recognition of formaldehyde by a cucurbit[10]uril-based porous supramolecular assembly incorporating adsorbed 1,8-diaminonaphthalene, *J. Mater. Chem. C*, 7 (2019) 1597-1603.

[14] R. H. Gao, L. X. Chen, Z. Tao. Development of hydroxylated cucurbit[n]urils, their derivatives and potential applications, *Coordin. Chem. Rev.*, 348 (2017) 1-24.

[15] R.-H. Gao, M. Liu, L.-X. Chen, X.-L. Ni, X. Xiao, H. Cong, Q.-J. Zhu, K. Chen, Z. Tao. *Angew Chemie Int. Ed*. 60 (2021) 15166-15191.

[16] D. Yang, M. Liu, X. Xiao, Z. Tao, C. Redshaw, *Coord. Chem. Rev*. 434 (2021) 213733.

[17] R.-L. Lin, J.-X, Liu, K. Chen, C. Redshaw, *Inorg. Chem. Front.*, *7* (2020) 3217-3246.

[18] A. P. Davis, in Comprehensive Supramolecular Chemistry II, Ed. J. L. Atwood, Elsevier, (2017).

[19] (a) Z. Gao, D. Bai, L. Chen, Z. Tao, X. Xiao, T. J. Prior, C. Redshaw, *RSC Adv*. *7* (2017) 461-467; (b) H. Feng, J. Kan, C. Redshaw, B. Bian, Z. Tao, X. Xiao, *Supramol. Chem.* 31 (2019) 260-267; (c) W. Xu; J. Kan; C. Redshaw; B. Bian; Y. Fan; Z. Tao, X. Xiao, *Supramol. Chem*. 31 (2019) 457-465; (d) Z. Xiao, Y. Zhou, W. Xu, T. J. Prior, B. Bian, C. Redshaw, X. Xiao, *New J. Chem*. *43*, (2019) 14938-14943; (e) P.-H. Shan, J.-L. Kan, X.-Y. Deng, C. Redshaw, B. Bian, Y. Fan, Z. Tao, X. Xiao, *Spectrochim. Acta A: Mol. Biomol. Spectrosc.*, 233 (2020) Article 118177; (f) W. Xu, X. Deng, X. Xiao, B. Bian, Q. Chen, S. J. Dalgarno, Z. Tao, C. Redshaw, *New J. Chem*. 44 (2020) 4311 – 4318; (g) W. Xu, X. Zhu, B. Bian, X. Xiao, Z. Tao, C. Redshaw, *Chemistry*, 2 (2020) 262-273.

[20] See for example G. R. Newkome, D. L. Fishel, G. Swift and W. D. Emmons. *Org. Synth*. 50 (1970) 102.

[21] D. H. Macartney. Encapsulation of Drug Molecules by Cucurbiturils: Effects on their Chemical Properties in Aqueous Solution. *Isr. J. Chem*, 51 (2011) 600-615.

[22] S. Walker, R. Oun, F. J. McInnes, N. J. Wheate. The Potential of Cucurbit[*n*]urils

in Drug Delivery. *Isr. J. Chem*, 51 (2011): 616-624.

[23] (a) J. Dobkowsk, E. Kirkor- Kaminska, J. Koput, A. Siemiarczuk, *J. Lumin*., 27 (1982) 339-355; (b) J. Dobkowski, Z. R. Grabowski, J. Waluk, W. Kühnle, W. Rettig, C. Rulliére, W. Yang, J. Adamus, J. Gebicki, *Proc. Indian Acad. Sci. (Chem. Sci.)*, 104 (1992) 143-152; (c) T. Fujiwara, J.-K. Lee, M. Z. Zgierski, E. C. Lim, *Chem. Phys. Lett*. 481 (2009) 78–82.

[24] P. -H. Shan, J. -H. Hu, M. Liu, Z. Tao, X. Xiao, C. Redshaw. Progress in host-guest macrocycle/pesticide research: recognition, detection, release and application. *Coord. Chem. Rev.* (2022), in-press.

[25] Y. Luo, W. Zhang, M. X. Yang, X. H. Feng, C. Redshaw, Q. Li, Z. Tao. A Twisted Cucurbit[14]uril-based Fluorescent Supramolecular Polymer Mediated by Metal Ion, *Macromolecules*, 55 (2022) 1642-1646.

[26] W. Zhang, Y. Luo, J. Zhao, C. Zhang, X.-L. Ni, Z. Tao. Controllable fabrication of a supramolecular polymer incorporating twisted cucurbit[14]uril and cucurbit[8]uril *via* self-sorting, *Chinese Chem. Lett.*, 33 (2022) 2455–2458.

[27] P.-H. Shan, J.-L. Kan, X.-Y. Deng, C. Redshaw, B. Bian, Y. Fan, Z. Tao. A fluorescent probe based on cucurbit[7]uril for the selective recognition of phenylalanine, *Spectrochim. Acta A: Mol. Biomol. Spectrosc.*, 233 (2020) 118177.

[28] W. Xu, J. Kan, B. Yang, T. J. Prior, B. Bian, Z. Tao, C. Redshaw. A study of the interaction between cucurbit[8]uril and alkylsubstituted 4-pyrrolidinopyridinium salts, *Chem. Asian J.*, 14 (2019) 235-242.

[29] Z.-Z. Gao, J. Kan, Z. Tao, B. Bian. A Stimuli-Responsive Supramolecular Assembly between Inverted cucurbit[7]uril and Hemicyanine Dye, *New J. Chem.*, 42 (2018) 15420 - 15426

[30] (a) Y. Matsushita, T. Hikida, *Chem. Phys. Lett*. 290 (1998) 349-354; (b) Y. Matsushita, T. Suzuki, T. Ichimura, T. Hikida, *Chem. Phys*., 286 (2003) 399–407.

[31] Y. Matsushita, T. Hikida, Chem. Phys. Lett. 290 (1998) 349.

[32] X. K. Fang, P. Kogerler, L. Isaacs, Cucurbit[*n*]uril-Polyoxoanion Hybrids. J. Am. Chem. Soc. 131 (2009) 432-433.

[33] O. V. Dolomanov, L. J. Bourhis, R. J. Gildea, J. A. K. Howard, H. Puschmann,

OLEX2: a complete structure solution, refinement and analysis program, *J. Appl. Cryst*. 42 (2009) 339-341.

Figures for the SI:

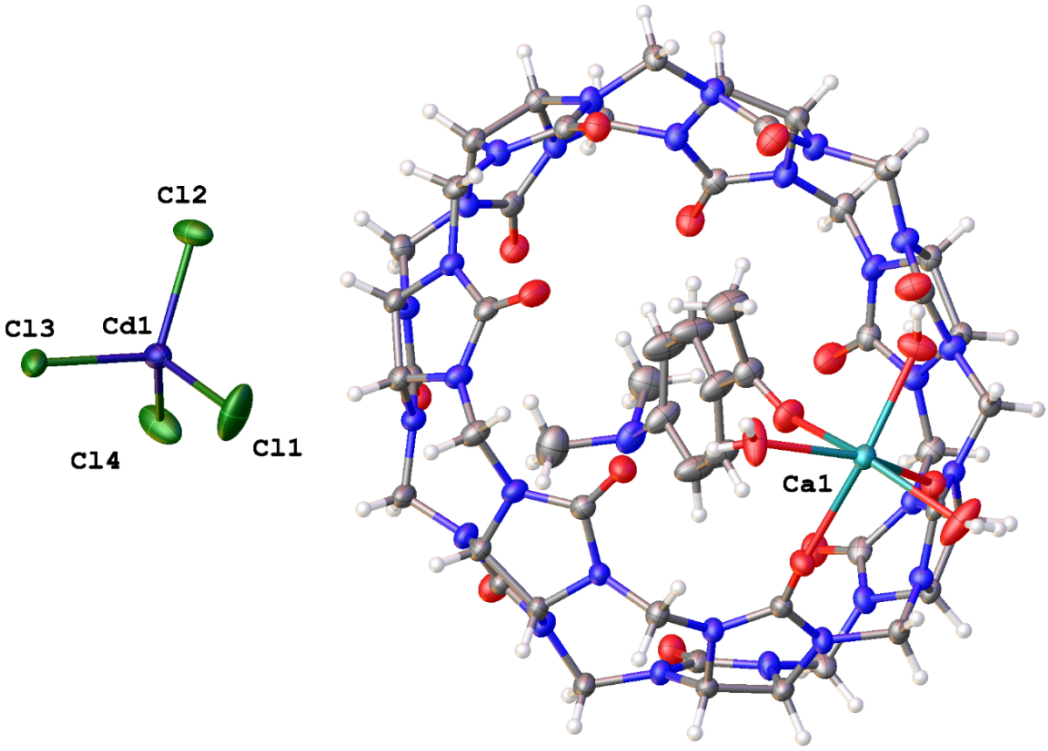

Figure S1. Asymmetric unit of Q[7]-DAPE with atoms drawn as 30 % probability ellipsoids. For clarity, minor disorder in the guest molecule is not shown.

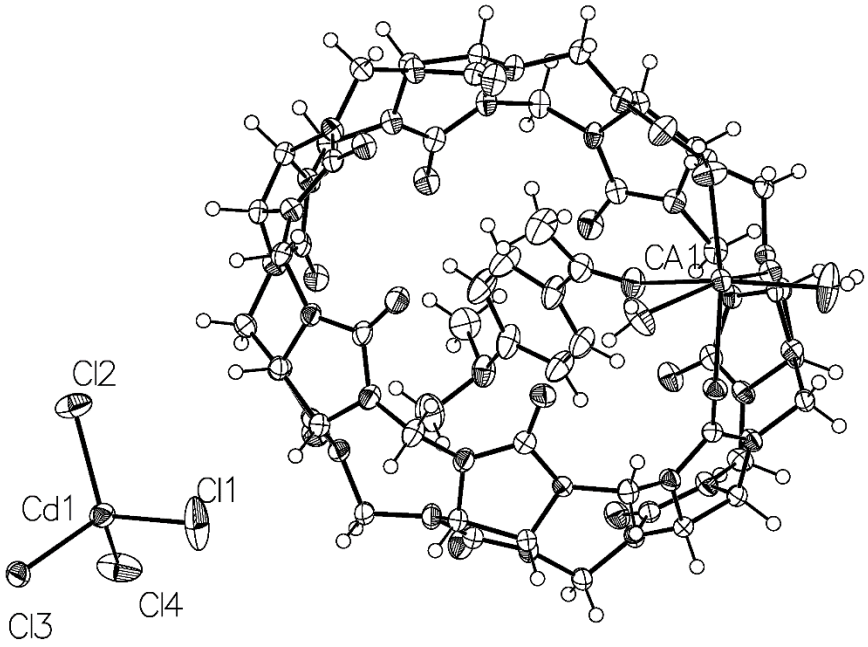

Figure S2. ORTEP style representation of the asymmetric unit of Q[7]-DAPE with atoms drawn as 30 % probability ellipsoids. For clarity, minor disorder in the guest molecule is not shown.

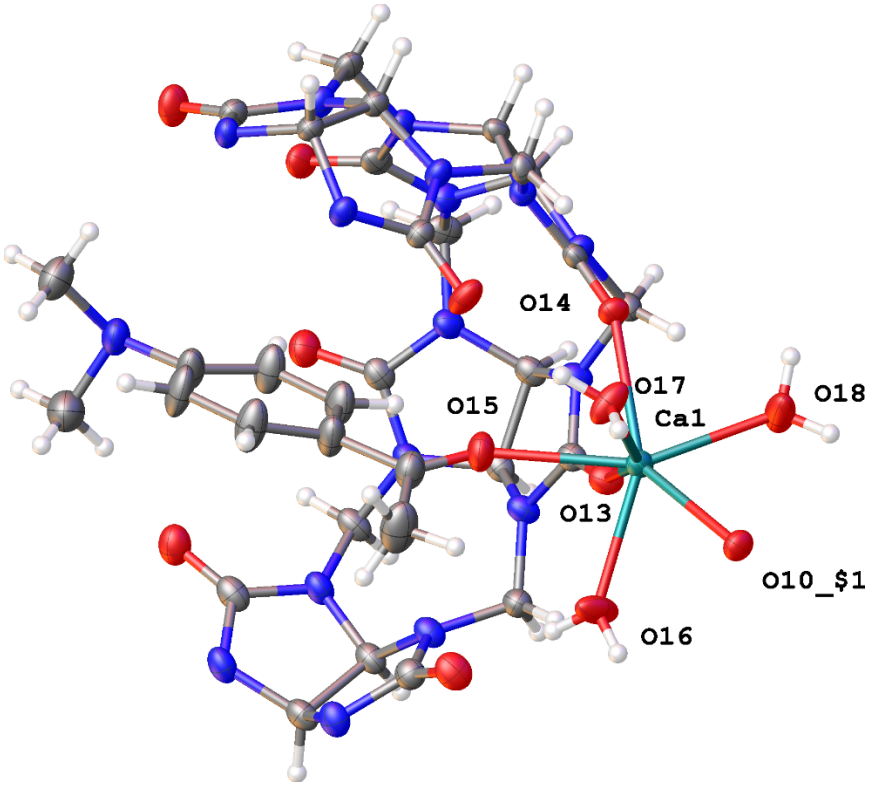

Figure S3. Portion of the asymmetric unit showing the coordination about Ca1. atoms drawn as 30 % probability ellipsoids. For clarity, minor disorder in the guest molecule is not shown. (symmetry operation \$1 = 1−*x*, 1−*y*, 1−*z*).

Graphic for TOC: